Evolutionary Context of Non–Sorbitol-Fermenting Shiga Toxin–Producing *Escherichia coli* O55:H7

Kyle Schutz, Lauren A. Cowley, Sharif Shaaban, Anne Carroll, Eleanor McNamara, David L. Gally, Gauri Godbole, Claire Jenkins, Timothy J. Dallman

In July 2014, an outbreak of Shiga toxin–producing *Escherichia coli* (STEC) O55:H7 in England involved 31 patients, 13 (42%) of whom had hemolytic uremic syndrome. Isolates were sequenced, and the sequences were compared with publicly available sequences of *E. coli* O55:H7 and O157:H7. A core-genome phylogeny of the evolutionary history of the STEC O55:H7 outbreak strain revealed that the most parsimonious model was a progenitor enteropathogenic O55:H7 sorbitol-fermenting strain, lysogenized by a Shiga toxin (Stx) 2a–encoding phage, followed by loss of the ability to ferment sorbitol because of a non-sense mutation in *srlA*. The parallel, convergent evolutionary histories of STEC O157:H7 and STEC O55:H7 may indicate a common driver in the evolutionary process. Because emergence of STEC O157:H7 as a clinically significant pathogen was associated with acquisition of the Stx2a-encoding phage, the emergence of STEC O55:H7 harboring the *stx2a* gene is of public health concern.

The first outbreak of Shiga toxin–producing *Escherichia coli* (STEC) O55:H7 in the United Kingdom occurred in the county of Dorset, England, in July 2014 (*1*). Ultimately, 31 cases were linked to the outbreak, and 13 (42%) of those patients had hemolytic uremic syndrome (HUS). Of the 13 with HUS, 8 (66%) had neurologic complications and 11 (90%) required prolonged treatment for kidney replacement. After enhanced epidemiologic surveillance and analysis of the patients' food, exposure, and travel histories, the only epidemiologic link identified was living in or having close links to Dorset County. Extensive microbiological investigations included testing of the environment, nondomestic animals, and household pets. Although no causal link was established, whole-genome sequencing and epidemiologic analyses were indicative of a local endemic zoonotic source (*1*).

Author affiliations: Public Health England Colindale, London, UK (K. Schutz, L.A. Cowley, G. Godbole, C. Jenkins, T.J. Dallman); The University of Edinburgh, Midlothian, UK (S. Shaaban, D.L. Gally); Cherry Orchard Hospital, Dublin, Ireland (A. Carroll, E. McNamara)

DOI: https://doi.org/10.3201/eid2312.170628

Previous studies postulated that the common STEC O157:H7 clone evolved from enteropathogenic *E. coli* (EPEC) serotype O55:H7 (*2*,*3*). Evolutionary models predict the stepwise acquisition of a Shiga toxin (Stx)–encoding bacteriophage in the EPEC O55:H7 progenitor strain, followed by the substitution of the *rfb* locus encoding the somatic O55 antigen with that encoding the O157 antigen, the acquisition of the pO157 plasmid, loss of the ability to ferment sorbitol, and loss of the ability to produce β-glucuronidase (*3*–*6*). Analyses from more recent studies have indicated that the Stx-encoding phage is an unstable evolutionary marker, with frequent acquisition and loss occurring in STEC O55:H7 and all 3 lineages of STEC O157 throughout their evolutionary history (*7*,*8*).

STEC O157:H7 has multiple genetic and phenotypic features that contribute to its pathogenicity or are used for detection and identification. The primary virulence factor defining the STEC group is production of Stx1, Stx2, or both. The genes encoding the toxins, *stx1* and *stx2*, are harbored on lambdoid prophage and are the targets of commercial and in-house diagnostic PCR assays (*9*). Both toxins can be divided into several subtypes, Stx1a–1d and Stx2a–2g (*10*). The locus of enterocyte effacement (LEE) is a 35-kb pathogenicity island encoding a type III secretion system (T3SS) responsible for the attaching and effacing phenotype that facilitates successful colonization of the human gut (*11*). The inability to ferment sorbitol or to produce β-glucuronidase differentiates STEC O157 from ≈90% of other gastrointestinal bacteria (*5*,*12*). These characteristics, along with resistance to tellurite, facilitate the detection and identification of STEC O157:H7 on selective media. The pO157 plasmid encodes multiple putative virulence factors, including enterohemolysin (*ehxA*) and an adhesin (*toxB*) (*13*).

The STEC O55:H7 Dorset outbreak strain shared certain characteristics with the STEC O157:H7 clone. Initial PCRs detected the presence of *stx2* and the intimin gene

eae, a marker for *E. coli* attaching and effacing phenotype; non–sorbitol-fermenting colonies of STEC O55 were identified after culture on sorbitol MacConkey agar (*1*,*9*). However, unlike the STEC O157 clone, the STEC O55 Dorset outbreak strain exhibited β-glucuronidase activity and was sensitive to tellurite. Laboratory records held at the Gastrointestinal Bacterial Reference Unit of Public Health England showed that this highly pathogenic strain had not previously been isolated from humans or animals in the United Kingdom. Our goal with this study was to identify the genetic determinants responsible for the phenotypic characteristics of the STEC O55:H7 Dorset outbreak strain and to explore the strain's evolutionary history.

Materials and Methods

Bacterial Strains

We studied 26 isolates of STEC O55:H7 from the outbreak, 10 isolates of STEC O55:H7 from Ireland, and 79 isolates selected to represent of the broad phylogeny of STEC O157:H7 (online Technical Appendix Table, https://wwwnc.cdc.gov/EID/article/23/12/17-0628-Techapp1.pdf). From public databases, we retrieved 10 genome sequences for *E. coli* O55:H7 and 2 for STEC O157:H7 (*6*,*7*,*14*,*15*) (Table 1).

Whole-Genome Sequencing, Assembly, and Alignment

We sequenced all isolates by using an Illumina paired-end (100-bp) protocol (https://www.illumina.com) and assembled them by using SPAdes Genome Assembler version 3.1.1 (*18*). The assemblies were annotated by using Prokka version 1.0.1 (*19*). We used the MinION (https://nanoporetech.com/products/minion) nanopore platform to sequence an isolate from the outbreak, designated 122262. A hybrid Illumina/MinION de novo assembly of 122262 constructed by using SPAdes yielded 15 contigs with the largest contig spanning the first 2.4 mbp. We aligned published reference genomes against the outbreak reference strain 122262 by using Mauve (*20*).

Genome, Plasmid, and Bacteriophage Comparisons

We retrieved from GenBank published nucleotide sequences of key virulence genes associated with toxicity, host-cell adhesion, and metabolic activity and concatenated in FASTA (http://www.ebi.ac.uk/Tools/sss/fasta/) file format. To determine the presence and absence of the gene panel, we performed a blastn (*21*) comparison against the extracted coding sequences of 122262. Significant hits were defined as those with a nucleotide identity of ≥90% over at least 90% of the query sequence. Truncated sequences were defined as matches with <90% coverage. We uploaded assembled data from the strains in FASTA file format to the PHAge Search Tool (PHAST) web server for prophage identification (*22*). Prophage region detection, prophage annotation, and circular genomic views from PHAST results were used along blast ring image generator (BRIG) plots (*23*) to isolate the prophage regions of 122262 and nucleotide homologies to the prophages in the Sakai reference genome (*16*). BRIG was used to visually compare the similarities between the Sakai and outbreak strain prophages. We compared prophage regions of 122262 with those extracted and analyzed by Shaaban et al. (*17*) by using the pipeline and strains presented in their study.

Phylogenetic Analyses

Short reads were quality trimmed (*24*) and mapped to the STEC O157:H7 Sakai reference genome (GenBank accession no. BA000007) by using Burrows-Wheeler aligner–maximal exact matching (*25*). We sorted and indexed the sequence alignment map output from the Burrows-Wheeler aligner to produce a binary alignment map by using SAMtools (*25*). GATK2 (*26*) was used to create a variant call format file from each of the B binary alignment maps, which were further parsed to extract only single-nucleotide polymorphism (SNP) positions that were of high quality (mapping quality >30, coverage of reads that passed quality metrics >10, variant ratio >0.9). We used pseudosequences of polymorphic positions to create maximum-likelihood trees by using RAxML (*27*). FASTQ (https://www.ncbi.nlm.nih.gov/pmc/

Table 1. *Escherichia coli* O55:H7 genome sequences retrieved from publicly available databases*

Name	Accession no.	Serotype	STX	SOR	GUD	Reference
USDA 5905	SRS702210	O55	–	+	+	(*7*)
3256–97–1	AEUA01000000	O55	–	+	+	(*7*)
RM12579–1	CP003109	O55	–	+	+	(*7*)
CB9615	NC_013941	O55	–	+	+	(*10*)
ZH-1141	Pending	O55:H7	–	+	+	(*14*)
2013C-4465	GCA_001644745.1	O55	Stx1a	+	+	(*15*)
Sakai		O157:H7	Stx1a and 2a	–	–	(*16*)
155	CP018237	O157:H7	Stx2a	–	–	(*17*)
TL-000142	ERR180875	O55	–	+	+	This study
SRR3578942	SRR3578942	O55:H7	Stx2d	+	+	This study
TL-000132	ERR197199	O55	–	+	+	This study
3041–1_85	ERR197201	O55	–	+	+	This study
100446	ERR178176	O55:H7	–	+	+	This study

*GUD, β-glucuronidase; SOR, sorbitol; Stx, Shiga toxin; –, negative; +, positive.

articles/PMC2847217/) sequences were deposited in the National Center for Biotechnology Information Short Read Archive under the BioProject PRJNA248042.

Results

General Genomic Features

STEC O55:H7 strain 122262 had a 5,364,131-bp chromosome and a 67,247-bp single plasmid of replicon type FIB-15. Use of blastn to compare the extracted plasmid sequence from 122262 with publicly available plasmid sequences belonging to CB9615, 2013C-4465, and Sakai indicated that the plasmid of 122262 was 99% identical to pO55 CB9615 over its complete length. Unlike pO157 in STEC O157:H7, the O55:H7 plasmids did not encode toxin B (*toxB*) or the enterohemolysin operon (*ehxABCD*). The *E. coli* O55:H7 strains 122262, CB9615, and 2013C-4465 did, however, encode a remote *toxB* homologue *efa1*/*lifA* on the chromosome that has 29% nt identity (97% coverage) with pO157 *toxB*. The LEE was inserted into the chromosome of strain 122262 at *tRNA-selC*, the most common insertion site in a range of pathogenic *E. coli* chromosomal backgrounds (*28*). Antimicrobial drug resistance determinants included *aadA-1b* encoding resistance to streptomycin and *dfrA-1* encoding resistance to trimethoprim.

Prophage Composition of 122262

PHAST identified 15 prophage interruptions in 122262, of which 5 were homologous in nucleotide identity to Sp2, Sp3, Sp6, Sp8, and Sp14 found in Sakai (*16*) (Table 2; Figure 1). Unique genetic content and position was found for 9 putative prophages (Figure 1). In addition, a Stx2a-encoding phage was identified at the Stx-associated bacteriophage insertion site *yecE* in strain 122262. In Sakai, the Stx1a (Sp15) and Stx2a (Sp5) encoding phages are inserted at *wrbA* and *yehV*, respectively. However, *yecE* is a known Stx-associated bacteriophage insertion site in strains of STEC O157:H7 encoding *stx2a* belonging to lineage Ic (*29*).

Long-read sequencing of 122262 facilitated comparison of the sequence of the Stx2a-encoding phage with other publicly available sequences of Stx2a-encoding phage. Shaaban et al. (*17*) compared prophage sequences for 14 strains of STEC O157:H7, including 8 Stx2a-encoding phages. Of the 8 Stx2a phages described in that study, 7 were closely related despite being found in globally distributed strains from different lineages. The sequence of the Stx2a-encoding phage from the outbreak strain, 122262, showed most similarity (>98% nt identity and >94% sequence coverage over the complete phage) with an outlier Stx2a-encoding phage designated 155, found in a subset of isolates of STEC O157 phage type 32 in lineage 1c, geographically associated with the island of Ireland (*17*,*29*) (Figure 2). The main difference between the 2 prophages was an insertion sequence element, a common source of prophage variation (Figure 2).

Sorbitol-Negative Phenotype of 122262

Like the common STEC O157:H7 clone, the STEC O55:H7 outbreak strain described in this study was characterized by its inability to ferment sorbitol. *srlA* and *srlE* encode components of a glucitol/sorbitol-specific phosphotransferase system. In STEC O157:H7, the sorbitol-negative phenotype was thought to have resulted from frameshifts in *srlA* and *srlE*, as observed in Sakai and EDL933 (*5*). SNP analysis of STEC O55:H7 122262 in our study revealed a non-sense mutation in *srlA* causing truncation of the last 29 aa, which was likely to reduce expression or produce a nonfunctional product. The sorbitol-negative phenotype, although a characteristic of STEC O157:H7, is rare in *E. coli* O55:H7 and has been described for only 1 other strain (RM12506, also referred to as BB2 and C523-03; genome not publicly available) (*7*,*30*).

Table 2. Location of prophages in Shiga toxin–producing *Escherichia coli* O55:H7 isolate 122262 from outbreak in Dorset County, England, July 2014, and related Sakai reference prophage*

Prophage in 122262	Location	Related Sakai phage	Identity, %
P1	298714–355267	Sp8	96
P2	2728769–2738381	NP	NA
P3	2958215–2992979	Sp3	98
P4	3119806–3151485	NP	NA
P5	3702030–3736837	Sp5	99
P6	4031314–4075190	NP	NA
P7	4166735–4223146	NP	NA
P8	4361295–4432383	Sp6	97
P9	4549353–4575262	NP	NA
P10	4662955–4712352	NP	NA
P11	4744636–4768829	NP	NA
P12	4868835–4901248	NP	NA
P13	5136256–5154117	NP	NA
P14	5221278–5261127	Sp14	98
P15	5287889–5361495	NP	NA
Stx-encoding phage	3607500–3655000	NP	NA

*NA, not applicable; NP, not present; Stx, Shiga toxin.

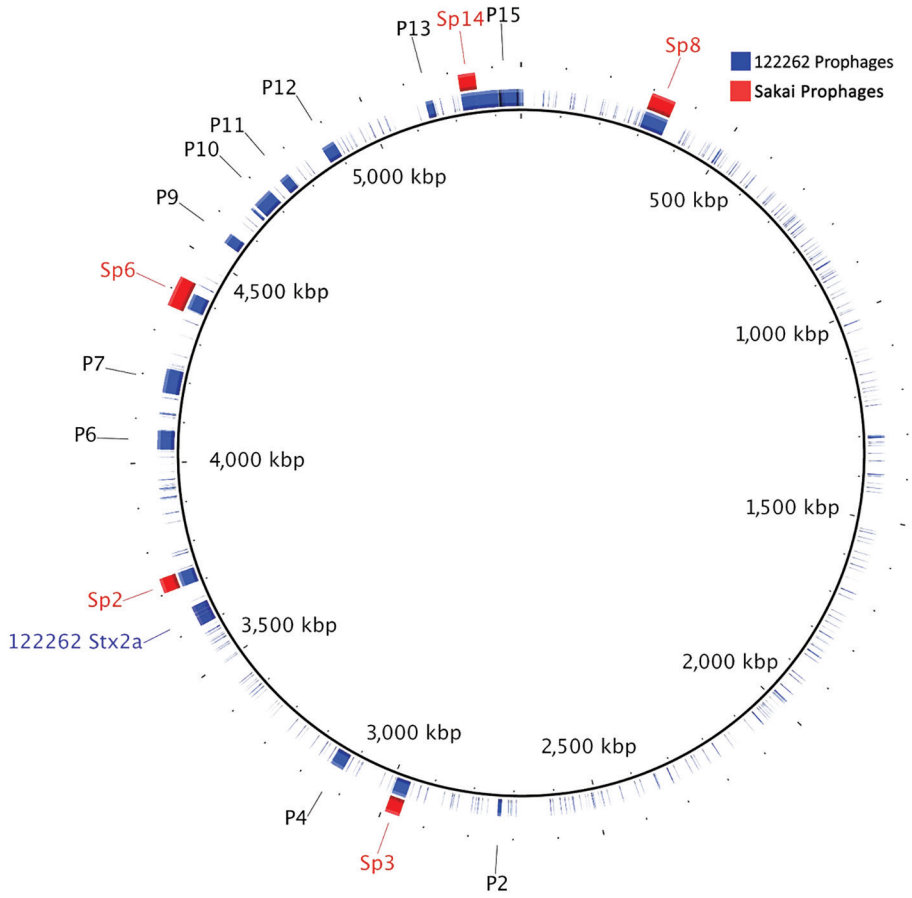

Figure 1. BLAST ring image generator (BRIG) plot generated from BLAST+ (*21*) comparisons of Shiga toxin–producing *Escherichia coli* (STEC) O55:H7 122262 prophages and homologous STEC O157:H7 Sakai prophages. STEC O55:H7 122262 chromosome is set as the reference genome, and the 122262 prophages (P1–P15) comprise the first ring. The homologous STEC O157:H7 Sakai prophages (Sp2, Sp3, Sp6, Sp8, and Sp14) identified in the BLAST analysis were added to the image according to their known locations (Table 2). Putative prophage sequence data were retrieved content from PHAge Search Tool (*22*) and plotted in BRIG.

β-Glucuronidase and Tellurite Phenotypes of 122262

β-glucuronidase is an inducible enzyme encoded by *uidA* and produced by ≈90% of pathogenic and nonpathogenic *E. coli*. The common STEC O157:H7 clone is a rare exception. The *uidA* loss of function mechanism in STEC O157:H7 was elucidated by Monday et al. (*31*) and included 2 frameshift mutations. The STEC O55:H7 outbreak strain 122262 had a β-glucuronidase–positive phenotype, and analysis of the genome by using MAUVE (*20*) did not identify any disruptive mutations in *uidA*. No β-glucuronidase–negative strains of *E. coli* O55:H7 have been described. Furthermore, the STEC O55 Dorset outbreak strain 122262 did not contain the *ter* cluster and was phenotypically sensitive to tellurite. As a consequence, it did not propagate when inoculated onto cefixime and tellurite sorbitol MacConkey agar and was not detected by routine culture methods used at the local hospital diagnostic microbiology laboratories in the United Kingdom (https://www.gov.uk/government/publications/smi-b-30-investigation-of-faecal-specimens-for-enteric-pathogens).

Phylogenetic Analyses

To investigate the evolutionary history of the STEC O55 Dorset outbreak strain, we constructed a core genome phylogeny (Figure 3). The analysis divided the sequences of the isolates in this study according to serotype; all isolates of *E. coli* O55:H7 clustered together on a separate branch of the tree, and all isolates of STEC O157:H7 clustered together on the branch below, regardless of sorbitol/β-glucuronidase phenotype or the presence of *stx* (Figure 3). The phylogenetic analysis of *E. coli* O55:H7 indicated that incorporation of the Stx-encoding prophage has occurred on multiple occasions within the EPEC O55:H7 background, with independent acquisition of *stx1* (*15*), *stx2d*, and *stx2a* into EPEC O55:H7. Likewise, multiple acquisition and loss events involving *stx1*, *stx2c, stx2a*, and less commonly *stx2d* have been described for STEC O157:H7 (*12*,*32*).

As noted by McFarland et al. (*1*), the outbreak strain was closely related to STEC O55:H7 *stx2a* isolates identified in Ireland during 2013–2014 (Figure 3). These 6 isolates from Ireland were <5 SNPs from the Dorset outbreak strain, indicating that the isolates from Ireland and Dorset County shared a common source (*8*). The outbreak strain had lost the ability to ferment sorbitol, which appears to be a recent adaption with all ancestral O55:H7, including those isolated in Ireland in 2012 retaining the ability to ferment sorbitol. A similar relationship exists between the sorbitol-positive and

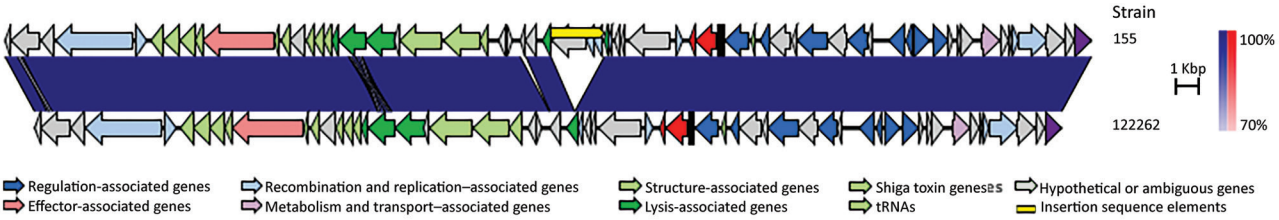

Figure 2. The sequence of the Stx2a-encoding phage from the July 2014 Dorset County, England, outbreak strain of Shiga toxin–producing *Escherichia* coli O55:H7, designated 122262, showed >98% nt identity with an outlier Stx2a-encoding phage designated 155, found in a subset of isolates of Shiga toxin–producing *Escherichia coli* O157 geographically associated with the island of Ireland. The main difference between the 2 prophages was an insertion sequence element.

sorbitol-negative STEC O157:H7 phenotypes; the sorbitol-negative phenotype is a more recent adaption from the sorbitol-positive progenitor strain (Figure 3) (*3*,*5*).

The most parsimonious model of evolution of the STEC O55:H7 Dorset outbreak strain was a progenitor EPEC O55:H7 sorbitol-fermenting strain lysogenized by an Stx2a-encoding phage and subsequent loss of the ability to ferment sorbitol. This stepwise model of evolution seems to mirror that seen in the common STEC O157:H7 clone; the acquisition of the STEC pathotype preceded phenotypic modulation.

Discussion

In the United Kingdom, STEC is regarded as a substantial threat to public health, and enhanced surveillance systems are in place (*32*). In England, HUS developed in ≈5% of symptomatic STEC O157:H7 patients (*33*), notably less than the 42% of patients in whom HUS developed during the STEC O55:H7 outbreak described in this study. The Dorset outbreak strain was closely related to the common STEC O157:H7 clone and shared several characteristics, most notably the presence of phage-encoded *stx2a*. Stx2a is associated with more severe symptoms, including the development of HUS, and it is probably the key virulence factor causing the high proportion of HUS cases in this outbreak (*10*). Of additional concern was the inability to detect the outbreak strain at the local hospital level by using the standard microbiology investigation method, cefixime and tellurite sorbitol MacConkey agar, because of this strain's sensitivity to tellurite.

A previously published stepwise evolutionary model showed the acquisition of *stx2* by a strain of EPEC O55:H7, resulting in emergence of a strain of STEC O55:H7, which was β-glucuronidase positive and sorbitol positive, closely related but ancestral to STEC O157:H7, which was β-glucuronidase positive and sorbitol positive (*34*). The loss of the sorbitol-positive phenotype in STEC O157:H7 was followed by the loss of β-glucuronidase expression, resulting in the common STEC O157 sorbitol-negative β-glucuronidase–negative clone. The evolutionary history of the Dorset outbreak strain begins with the EPEC O55:H7 progenitor strain described previously (*6*) (Figure 3). Subsequent acquisition of an Stx2a-encoding phage was confirmed by detection of STEC O55:H7 β-glucuronidase–positive sorbitol-positive isolates in Ireland in 2012 (Figure 3). The loss of the sorbitol-positive phenotype mirrored the genetic events proposed to have occurred in the evolution of STEC O157, albeit by an alternative mechanism.

The parallel, convergent evolutionary history of STEC O157:H7 and STEC O55:H7 may indicate a common driver in the evolutionary process. Adaptation to a new niche may be accompanied by modification of gene expression because genes no longer required for, or incompatible with, the variation in lifestyle are selectively inactivated by point mutation, insertion, or deletion (*35*). Loss of the sorbitol-positive phenotype may coincide with the successful colonization of a new animal host or the ability to transmit more effectively between animal hosts without the need to survive in the environment for long periods (*28*,*36*).

The detection of the STEC O55:H7 sorbitol-negative strain in patients in Ireland before the outbreak in Dorset led to speculation that ruminants (most likely cattle or sheep) on the island of Ireland were the source of the outbreak strain (*1*). Transmission between Ireland and Dorset may have occurred via movement of persons, livestock, or a secondary vector such as migratory birds (*37*). The finding that the Stx2a-encoding phage has a high level of similarity to Stx2a-encoding phage found in a previously described sublineage of STEC O157 PT32 geographically linked to Ireland may provide further evidence of the origin of this strain (*17*,*29*). Phages from STEC O157 may be exchanged with other phages from serotypes of *E. coli* in the gut of the ruminant host or in the environment. Analysis and comparison of phage sequences to provide clues regarding the origin of a strain of STEC is a novel approach to outbreak investigation; additional studies are required to evaluate the utility of the approach. Further work will be hampered by the lack of available sequences of the Stx-encoding phage and the difficulties with assembling the sequences because of the inability of short-read sequencing to resolve the large number of repetitive and paralogous features characteristic of the prophage.

Figure 3. Core genome phylogeny illustrating the evolutionary history of the Shiga toxin–producing *Escherichia coli* (STEC) O55 strain from the July 2014 Dorset County, England, outbreak in the context of STEC O157:H7 lineages I, II, and I/II.Scale bar indicates nucleotide substitutions per site.

The STEC O55:H7 Dorset outbreak strain described in this study shared characteristics with the common STEC O157:H7 clone, specifically the acquisition of an Stx2a-encoding phage and the sorbitol-negative phenotype. Key differences between the 2 strains include the *rfb* gene cluster, plasmid content, β-glucuronidase phenotype, and the absence of the *ter* gene cluster in the STEC O55:H7 outbreak strain. Despite these differences, this study provides evidence of parallel, convergent evolution of STEC O157:H7 and STEC O55:H7, involving multiple acquisitions of Stx-encoding phages and loss of the ability to ferment sorbitol. Previous studies have shown a clear association with STEC harboring *stx2a* and progression to HUS (*10*). Acquisition of the Stx2a-encoding phage seems to explain the emergence of STEC O157:H7 as a clinically significant pathogen; in contrast to the acquisition of *stx2c*, evidence suggests that after Stx2a-encoding phage is integrated in a population, it tends to be maintained and may be associated with higher excretions levels in cattle (*29*,*36*). As such, the emergence of STEC O55:H7 harboring *stx2a* is of public health concern.

Acknowledgments

We acknowledge all members of the Outbreak Control Team, especially Noeleen McFarland, Amy Mikhail, and Sooria Balasegaram.

This work was supported by the National Institute for Health Research Health Protection Research Unit in Gastrointestinal Infections. D.L.G., T.J.D., and S.S. were supported by a Food Standards Scotland/Food Standards Agency study grant (FS101055).

Mr. Schutz is a recent graduate of the London School of Hygiene and Tropical Medicine and the Royal Veterinary College in London. His research interests include emerging zoonoses and host adaptation.

References

1. McFarland N, Bundle N, Jenkins C, Godbole G, Mikhail A, Dallman T, et al. Recurrent seasonal outbreak of an emerging serotype of Shiga-toxin producing *Escherichia coli* (STEC O55:H7 stx 2a) in the South West of England, July 2014–September 2015. Euro Surveill. 2017;22:30610. 10.2807/1560-7917.ES.2017.22.36.30610
2. Whittam TS, Wolfe ML, Wachsmuth IK, Orskov F, Orskov I, Wilson RA. Clonal relationships among *Escherichia coli* strains that cause hemorrhagic colitis and infantile diarrhea. Infect Immun. 1993;61:1619–29.
3. Feng P, Lampel KA, Karch H, Whittam TS. Genotypic and phenotypic changes in the emergence of *Escherichia coli* O157:H7. J Infect Dis. 1998;177:1750–3. http://dx.doi.org/10.1086/517438
4. Iguchi A, Ooka T, Ogura Y. Asadulghani, Nakayama K, Frankel G, et al. Genomic comparison of the O-antigen biosynthesis gene clusters of *Escherichia coli* O55 strains belonging to three distinct lineages. Microbiology. 2008;154:559–70. http://dx.doi.org/10.1099/mic.0.2007/013334-0
5. Wick LM, Qi W, Lacher DW, Whittam TS. Evolution of genomic content in the stepwise emergence of *Escherichia coli* O157:H7. J Bacteriol. 2005;187:1783–91. http://dx.doi.org/10.1128/JB.187.5.1783-1791.2005
6. Zhou Z, Li X, Liu B, Beutin L, Xu J, Ren Y, et al. Derivation of *Escherichia coli* O157:H7 from its O55:H7 precursor. PLoS One. 2010;5:e8700. http://dx.doi.org/10.1371/journal.pone.0008700
7. Kyle JL, Cummings CA, Parker CT, Quiñones B, Vatta P, Newton E, et al. *Escherichia coli* serotype O55:H7 diversity supports parallel acquisition of bacteriophage at Shiga toxin phage insertion sites during evolution of the O157:H7 lineage. J Bacteriol. 2012;194:1885–96. http://dx.doi.org/10.1128/JB.00120-12
8. Dallman TJ, Byrne L, Ashton PM, Cowley LA, Perry NT, Adak G, et al. Whole-genome sequencing for national surveillance of Shiga toxin-producing *Escherichia coli* O157. Clin Infect Dis. 2015;61:305–12. http://dx.doi.org/10.1093/cid/civ318
9. Jenkins C, Lawson AJ, Cheasty T, Willshaw GA. Assessment of a real-time PCR for the detection and characterization of verocytotoxigenic *Escherichia coli.* J Med Microbiol. 2012;61:1082–5. http://dx.doi.org/10.1099/jmm.0.041517-0
10. Persson S, Olsen KE, Ethelberg S, Scheutz F. Subtyping method for *Escherichia coli* Shiga toxin (verocytotoxin) 2 variants and correlations to clinical manifestations. J Clin Microbiol. 2007; 45:2020–4. http://dx.doi.org/10.1128/JCM.02591-06
11. Stevens MP, Frankel GM. The locus of enterocyte effacement and associated virulence factors of enterohemorrhagic *Escherichia coli*. Microbiol Spectr. 2014;2:EHEC-0007–2013. http://dx.doi.org: 10.1128/microbiolspec.EHEC-0007-2013
12. Feng P, Lampel KA. Genetic analysis of uidA expression in enterohaemorrhagic *Escherichia coli* serotype O157:H7. Microbiology. 1994;140:2101–7. http://dx.doi.org/10.1099/13500872-140-8-2101
13. Lim JY, Yoon J, Hovde CJ. A brief overview of *Escherichia coli* O157:H7 and its plasmid O157. J Microbiol Biotechnol. 2010;20:5–14.
14. Mainda G, Lupolova N, Sikakwa L, Bessell PR, Muma JB, Hoyle DV, et al. Phylogenomic approaches to determine the zoonotic potential of Shiga toxin-producing *Escherichia coli* (STEC) isolated from Zambian dairy cattle. Sci Rep. 2016;6:26589. http://dx.doi.org/10.1038/srep26589
15. Lindsey RL, Rowe L, Garcia-Toledo L, Loparev V, Knipe K, Stripling D, et al. High-quality draft genome sequences for five non-o157 Shiga toxin-producing *Escherichia coli* strains generated with PacBio sequencing and optical maps. Genome Announc. 2016;4:e00626–16. http://dx.doi.org/10.1128/genomeA.00626-16
16. Hayashi T, Makino K, Ohnishi M, Kurokawa K, Ishii K, Yokoyama K, et al. Complete genome sequence of enterohemorrhagic *Escherichia coli* O157:H7 and genomic comparison with a laboratory strain K-12. DNA Res. 2001;8:11–22. http://dx.doi.org/10.1093/dnares/8.1.11
17. Shaaban S, Cowley LA, McAteer SP, Jenkins C, Dallman TJ, Bono JL, et al. Evolution of a zoonotic pathogen: investigating prophage diversity in enterohaemorrhagic *Escherichia coli* O157 by long-read sequencing. Microb Genom. 2016;2:e000096.
18. Bankevich A, Nurk S, Antipov D, Gurevich AA, Dvorkin M, Kulikov AS, et al. SPAdes: a new genome assembly algorithm and its applications to single-cell sequencing. J Comput Biol. 2012;19:455–77. http://dx.doi.org/10.1089/cmb.2012.0021
19. Seemann T. Prokka: rapid prokaryotic genome annotation. Bioinformatics. 2014;30:2068–9. http://dx.doi.org/10.1093/bioinformatics/btu153
20. Darling AE, Mau B, Perna NT. progressiveMauve: multiple genome alignment with gene gain, loss and rearrangement. PLoS One. 2010;5:e11147. http://dx.doi.org/10.1371/journal.pone.0011147
21. Altschul SF, Gish W, Miller W, Myers EW, Lipman DJ. Basic local alignment search tool. J Mol Biol. 1990;215:403–10. http://dx.doi.org/10.1016/S0022-2836(05)80360-2

22. Zhou Y, Liang Y, Lynch KH, Dennis JJ, Wishart DS. PHAST: a fast phage search tool. Nucleic Acids Res. 2011;39:W347–52.
23. Alikhan NF, Petty NK, Ben Zakour NL, Beatson SA. BLAST ring image generator (BRIG): simple prokaryote genome comparisons. BMC Genomics. 2011;12:402. http://dx.doi.org/10.1186/1471-2164-12-402
24. Bolger AM, Lohse M, Usadel B. Trimmomatic: a flexible trimmer for Illumina sequence data. Bioinformatics. 2014;30:2114–20. http://dx.doi.org/10.1093/bioinformatics/btu170
25. Li H, Durbin R. Fast and accurate long-read alignment with Burrows-Wheeler transform. Bioinformatics. 2010;26:589–95. http://dx.doi.org/10.1093/bioinformatics/btp698
26. McKenna A, Hanna M, Banks E, Sivachenko A, Cibulskis K, Kernytsky A, et al. The Genome Analysis Toolkit: a MapReduce framework for analyzing next-generation DNA sequencing data. Genome Res. 2010;20:1297–303. http://dx.doi.org/10.1101/gr.107524.110
27. Stamatakis A. RAxML version 8: a tool for phylogenetic analysis and post-analysis of large phylogenies. Bioinformatics. 2014;30:1312–3. http://dx.doi.org/10.1093/bioinformatics/btu033
28. Ingle DJ, Tauschek M, Edwards DJ, Hocking DM, Pickard DJ, Azzopardi KI, et al. Evolution of atypical enteropathogenic *E. coli* by repeated acquisition of LEE pathogenicity island variants. Nat Microbiol. 2016;1:15010. http://dx.doi.org/10.1038/nmicrobiol.2015.10
29. Dallman TJ, Ashton PM, Byrne L, Perry NT, Petrovska L, Ellis R, et al. Applying phylogenomics to understand the emergence of Shiga-toxin–producing *Escherichia coli* O157:H7 strains causing severe human disease in the UK. Microb Genom. 2015;1:e000029. http://dx.doi.org/10.1099/mgen.0.000029
30. Feng PC, Jinneman K, Scheutz F, Monday SR. Specificity of PCR and serological assays in the detection of *Escherichia coli* Shiga toxin subtypes. Appl Environ Microbiol. 2011;77:6699–702. http://dx.doi.org/10.1128/AEM.00370-11
31. Monday SR, Whittam TS, Feng PC. Genetic and evolutionary analysis of mutations in the *gusA* gene that cause the absence of beta-glucuronidase activity in *Escherichia coli* O157:H7. J Infect Dis. 2001;184:918–21. http://dx.doi.org/10.1086/323154
32. Sánchez S, Llorente MT, Herrera-León L, Ramiro R, Nebreda S, Remacha MA, et al. Mucus-activatable Shiga toxin genotype stx2d in *Escherichia coli* O157:H7. Emerg Infect Dis. 2017;23:1431–3. http://dx.doi.org/10.3201/eid2308.170570
33. Byrne L, Jenkins C, Launders N, Elson R, Adak GK. The epidemiology, microbiology and clinical impact of Shiga toxin-producing *Escherichia coli* in England, 2009–2012. Epidemiol Infect. 2015;143:3475–87. http://dx.doi.org/10.1017/S0950268815000746
34. Feng PC, Monday SR, Lacher DW, Allison L, Siitonen A, Keys C, et al. Genetic diversity among clonal lineages within *Escherichia coli* O157:H7 stepwise evolutionary model. Emerg Infect Dis. 2007;13:1701–6. http://dx.doi.org/10.3201/eid1311.070381
35. Maurelli AT. Black holes, antivirulence genes, and gene inactivation in the evolution of bacterial pathogens. FEMS Microbiol Lett. 2007;267:1–8. http://dx.doi.org/10.1111/j.1574-6968.2006.00526.x
36. Matthews L, Reeve R, Gally DL, Low JC, Woolhouse ME, McAteer SP, et al. Predicting the public health benefit of vaccinating cattle against *Escherichia coli* O157. Proc Natl Acad Sci U S A. 2013;110:16265–70. http://dx.doi.org/10.1073/pnas.1304978110
37. See comment in PubMed Commons belowPersad AK, LeJeune JT. Animal reservoirs of Shiga toxin-producing *Escherichia coli*. Microbiol Spectr. 2014;2:EHEC-0027–2014.

Address for correspondence: Claire Jenkins, Gastrointestinal Bacteria Reference Unit, Public Health England, 61 Colindale Ave, NW9 5HT, UK; email: claire.jenkins@phe.gov.uk

EID Podcast:
Emerging Infectious Diseases Cover Art

Byron Breedlove, managing editor of the journal, elaborates on aesthetic considerations and historical factors, as well as the complexities of obtaining artwork for *Emerging Infectious Diseases*.

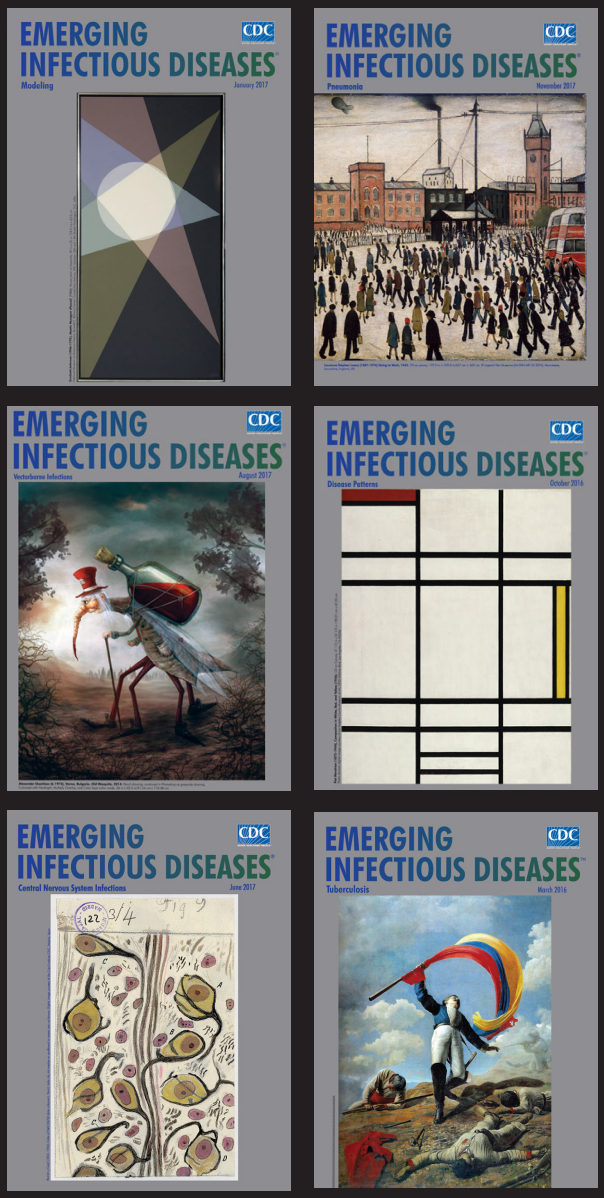

Visit our website to listen:

EMERGING INFECTIOUS DISEASES

https://www2c.cdc.gov/podcasts/player.asp?f=8646224

Article DOI: https://doi.org/10.3201/eid2312.170628

Evolutionary Context of Non–Sorbitol-Fermenting Shiga Toxin–Producing *Escherichia coli* O55:H7

Technical Appendix

Technical Appendix Table. Genomic analysis of 26 isolates of STEC O55:H7 from the July 2014 outbreak in Dorset County, England; 10 isolates of STEC O55:H7 from Ireland, and 79 isolates selected to represent of the broad phylogeny of STEC O157:H7*

ACCESSION	SEROGROUP	STX	SOR	GUD	ANNOTATION
ERR178176	O55	–	+	+	100446 SOR+ GUD+
GCA_001644745.1	O55	stx1a	+	+	2013C–4465 SOR+ GUD+ Stx1a
ERR180875	O55	–	+	+	TL–000142 SOR+ GUD+
NC_013941	O55	–	+	+	CB9615 SOR+ GUD+
ADMX01000000	O157	stx2a	–	–	Lineage I
AKLW01000000	O157	stx1/2a/2c	–	–	Lineage I
AKLY01000000	O157	stx2c	–	–	Lineage I
AKMN01000000	O157	stx2c	–	–	Lineage I
SRR1984083	O157	stx2c	–	–	Lineage I
SRR4180231	O157	stx2c	–	–	Lineage I
SRR5904129	O157	stx2a/2c	–	–	Lineage I
SRR2034057	O157	stx1a/2c	–	–	Lineage I
SRR5024451	O157	stx2c	–	–	Lineage I
SRR5904130	O157	stx2a	–	–	Lineage I
SRR2187202	O157	stx2a/2c	–	–	Lineage I
SRR2187203	O157	stx2a/2c	–	–	Lineage I
SRR1981319	O157	stx2c	–	–	Lineage I
SRR1981361	O157	stx2c	–	–	Lineage I
SRR1981368	O157	stx2c	–	–	Lineage I
SRR1981423	O157	stx2c	–	–	Lineage I
SRR4176979	O157	stx2c	–	–	Lineage I
SRR4180824	O157	stx2c	–	–	Lineage I
SRR4184846	O157	stx2a	–	–	Lineage I
SRR4786402	O157	stx2a/2c	–	–	Lineage I
SRR4788235	O157	stx2a	–	–	Lineage I
SRR4788323	O157	stx2a	–	–	Lineage I
SRR5005300	O157	stx2c	–	–	Lineage I
SRR5006372	O157	stx1a/2c	–	–	Lineage I
SRR5024199	O157	–	–	–	Lineage I
SRS932722	O157	stx1/2a/2c	–	–	Lineage I
Not available	O157	stx1a/2c	–	–	Lineage I/II
SRR5904105	O157	stx1a/2c	–	–	Lineage I/II
SRR1981384	O157	stx2a/2c	–	–	Lineage I/II
SRR2034081	O157	stx1a/2c	–	–	Lineage I/II
SRR4787234	O157	stx2c	–	–	Lineage I/II
SRR4787274	O157	stx1a/2c	–	–	Lineage I/II
SRR4788195	O157	stx2c	–	–	Lineage I/II
SRR4897273	O157	stx1a/2c	–	–	Lineage I/II
AKKY01000000	O157	stx1a/2c	–	–	Lineage II
AKLA01000000	O157	stx1a/2c	–	–	Lineage II
SRR5905734	O157	stx2c	–	–	Lineage II
SRR5905747	O157	stx2c	–	–	Lineage II
SRR5018342	O157	–	–	–	Lineage II
SRR5904104	O157	stx2c	–	–	Lineage II
SRR1980985	O157	stx2c	–	–	Lineage II
SRR1981377	O157	stx2c	–	–	Lineage II
SRR1981397	O157	stx2c	–	–	Lineage II
SRR1981716	O157	stx2c	–	–	Lineage II
SRR2034093	O157	stx2c	–	–	Lineage II
SRR4177018	O157	stx2c	–	–	Lineage II

ACCESSION	SEROGROUP	STX	SOR	GUD	ANNOTATION
SRR4181527	O157	stx2c	–	–	Lineage II
SRR4184741	O157	stx2c	–	–	Lineage II
SRR4192121	O157	stx2a/2c	–	–	Lineage II
SRR4195486	O157	stx2c	–	–	Lineage II
SRR4195749	O157	stx2c	–	–	Lineage II
SRR4195765	O157	stx2a/2c	–	–	Lineage II
SRR4195765	O157	stx2a/2c	–	–	Lineage II
SRR4787238	O157	stx2a/2c	–	–	Lineage II
SRR4787292	O157	stx2c	–	–	Lineage II
SRR4787855	O157	stx2c	–	–	Lineage II
SRR4787900	O157	stx2c	–	–	Lineage II
SRR4787906	O157	stx2c	–	–	Lineage II
SRR4788210	O157	stx1a/2c	–	–	Lineage II
SRR4788290	O157	stx2c	–	–	Lineage II
SRR4897337	O157	stx1a/2c	–	–	Lineage II
SRR4897491	O157	–	–	–	Lineage II
SRR4897542	O157	stx2c	–	–	Lineage II
SRR5005528	O157	stx2c	–	–	Lineage II
SRR5006048	O157	stx2c	–	–	Lineage II
SRR5006078	O157	stx2c	–	–	Lineage II
SRR5006435	O157	stx2a/2c	–	–	Lineage II
SRR5017542	O157	–	–	–	Lineage II
SRR5024243	O157	–	–	–	Lineage II
SRR5024250	O157	stx2c	–	–	Lineage II
SRR5024470	O157	stx2c	–	–	Lineage II
SRR5024504	O157	stx2c	–	–	Lineage II
CP003109	O55	–	+	+	RM12579 SOR+ GUD+
SRR2034251	O157	stx2c	–	–	SOR–GUD– Stx2c
SRR4897272	O157	stx2c	–	–	SOR– GUD– Stx2c
SRR5033648	O55	–	–	+	SOR– GUD+ Stx2a Ireland
SRR5033651	O55	–	–	+	SOR– GUD+ Stx2a Ireland
SRR5033665	O55	–	–	+	SOR– GUD+ Stx2a Ireland
SRR5033691	O55	–	–	+	SOR– GUD+ Stx2a Ireland
SRR5033692	O55	–	–	+	SOR– GUD+ Stx2a Ireland
SRR5033714	O55	–	–	+	SOR– GUD+ Stx2a Ireland
SRR3241858	O55	stx2a	–	+	SOR– GUD+ Stx2a Outbreak
SRR5904128	O55	stx2a	–	+	SOR– GUD+ Stx2a Outbreak
SRR5023697	O55	stx2a	–	+	SOR– GUD+ Stx2a Outbreak
SRR3240983	O55	stx2a	–	+	SOR– GUD+ Stx2a Outbreak
SRR3240985	O55	stx2a	–	+	SOR– GUD+ Stx2a Outbreak
SRR3240986	O55	stx2a	–	+	SOR– GUD+ Stx2a Outbreak
SRR3241097	O55	stx2a	–	+	SOR– GUD+ Stx2a Outbreak
SRR3241840	O55	stx2a	–	+	SOR– GUD+ Stx2a Outbreak
SRR3241843	O55	stx2a	–	+	SOR– GUD+ Stx2a Outbreak
SRR3241872	O55	stx2a	–	+	SOR– GUD+ Stx2a Outbreak
SRR3242000	O55	stx2a	–	+	SOR– GUD+ Stx2a Outbreak
SRR3242001	O55	stx2a	–	+	SOR– GUD+ Stx2a Outbreak
SRR3578577	O55	stx2a	–	+	SOR– GUD+ Stx2a Outbreak
SRR3578601	O55	stx2a	–	+	SOR– GUD+ Stx2a Outbreak
SRR3581428	O55	stx2a	–	+	SOR– GUD+ Stx2a Outbreak
SRR5023710	O55	stx2a	–	+	SOR– GUD+ Stx2a Outbreak
SRR5023715	O55	stx2a	–	+	SOR– GUD+ Stx2a Outbreak
SRR5023716	O55	stx2a	–	+	SOR– GUD+ Stx2a Outbreak
SRR5023727	O55	stx2a	–	+	SOR– GUD+ Stx2a Outbreak
SRR5023769	O55	stx2a	–	+	SOR– GUD+ Stx2a Outbreak
SRR5023782	O55	stx2a	–	+	SOR– GUD+ Stx2a Outbreak
SRR5023783	O55	stx2a	–	+	SOR– GUD+ Stx2a Outbreak
SRR5023789	O55	stx2a	–	+	SOR– GUD+ Stx2a Outbreak
SRR5023803	O55	stx2a	–	+	SOR– GUD+ Stx2a Outbreak
SRR5023932	O55	stx2a	–	+	SOR– GUD+ Stx2a Outbreak
SRR5024312	O55	stx2a	–	+	SOR– GUD+ Stx2a Outbreak
SRR4897293	O157	stx2c	–	+	SOR– GUD+ Stx2c
SRR5017532	O157	stx2c	–	+	SOR– GUD+ Stx2c
SRR5018181	O157	stx2c	–	+	SOR– GUD+ Stx2c
AEUA01000000	O55	–	+	+	SOR+ GUD+
SRR4179257	O55	–	+	+	SOR+ GUD+ Ireland
SRR2187155	O157	stx2a	+	+	SOR+ GUD+ Stx2a
SRR5280511	O157	stx2a	+	+	SOR+ GUD+ Stx2a
SRR5904106	O55	stx2a	+	+	SOR+ GUD+ Stx2a Ireland

ACCESSION	SEROGROUP	STX	SOR	GUD	ANNOTATION
SRR5904127	O107	stx2a	+	+	SOR+ GUD+ Stx2a Ireland
SRR5033689	O55	–	+	+	SOR+ GUD+ Stx2a Ireland
SRR5033719	O55	–	+	+	SOR+ GUD+ Stx2a Ireland
SRR3578942	O55	stx2d	+	+	SOR+ GUD+ Stx2d
ERR197201	O55	–	+	+	TL–000132 SOR+ GUD+
ERR197199	O55	–	+	+	TL–000142 SOR+ GUD+
SRS702210	O55	–	+	+	USA 5905 SOR+ GUD+
ERR1138642	O55	–	+	+	ZH–1141 SOR+ GUD+

*GUD, β-glucuronidase; SOR, sorbitol; STEC, Shiga toxin–producing *Escherichia coli*; stx, Shiga toxin.